The effects of interactive ozone chemistry on simulations of the middle atmosphere

F. Sassi, B. A. Boville, D. Kinnison, and R. R. Garcia
National Center for Atmospheric Research, Boulder, Colorado, USA

Received 1 December 2004; revised 11 March 2005; accepted 18 March 2005; published 13 April 2005.

[1] We compare two simulations of the middle atmosphere using the NCAR Whole Atmosphere Community Climate Model, which includes a comprehensive middle atmosphere chemistry model. Ozone is fully interactive in the first simulation. A zonal mean and monthly mean ozone climatology is constructed from the interactive simulation. That ozone climatology is used to determine the radiative heating rates in the second simulation. Comparison of the two simulations shows that using the zonal-mean ozone climatology significantly affects the climate of the middle atmosphere. Differences between the two simulations are statistically significant throughout the tropics in the upper stratosphere and lower mesosphere. **Citation:** Sassi, F., B. A. Boville, D. Kinnison, and R. R. Garcia (2005), The effects of interactive ozone chemistry on simulations of the middle atmosphere, *Geophys. Res. Lett.*, *32*, L07811, doi:10.1029/2004GL022131.

1. Introduction

[2] Assessment of climate change and variability in the middle atmosphere, and attempts to distinguish man-made from natural phenomena have motivated the development and scientific application of general circulation models with interactive chemistry in the last few years [*World Meteorological Organization* (*WMO*), 2003]. While assessment of model climatology is a standard practice, little attention has been paid to the effects of interactive ozone chemistry on the simulated climate of the middle atmosphere. The impact on the simulated climate when ozone is calculated interactively instead of being imposed as a fixed (climatological) field has not been systematically investigated before.

[3] In this study, we report two simulations carried out with the NCAR Whole Atmosphere Community Climate Model (WACCM), version 2. The model is described in Section 2. In the first simulation, the computed ozone field is used in the calculation of shortwave heating rates. The ozone climatology obtained from this simulation is presented in Section 3, along with a comparison to UARS observations. A second simulation is then carried out with a fixed ozone climatology used in the radiative heating calculations. Section 4 illustrates changes in climate between the two simulations. Section 5 gives a summary and conclusions.

2. Model Description

[4] WACCM, version 2, is based on the NCAR Community Atmosphere Model, version 3 (CAM3; see http://www.ccsm.ucar.edu/models/atm-cam/index.html). WACCM2 uses the lower atmospheric parameterizations and processes from a preliminary version of CAM3, which differs only in the details of the cloud fraction calculation and adjustable constants from the final CAM3. Transport and dynamics are solved using the finite-volume scheme of *Lin* [2005] at $2^\circ \times 2.5^\circ$ (latitude by longitude) horizontal resolution. WACCM2 has 66 vertical levels from the ground to about 150 km. Above about 60 km, parameterizations and physical processes beyond those present in CAM3 are included to better represent the mesosphere and lower thermosphere [*Sassi et al.*, 2002, 2004].

[5] The chemistry module used in WACCM2 is based on the Model for Ozone and Related chemical Tracers, version 3 [see *Park et al.*, 2004]. WACCM2 incorporates a 50 species mechanism that includes the O_x, NO_x, HO_x, ClO_x, and BrO_x chemical families, along with tropospheric source species (CH_4, N_2O, CFCs, HCFCs, halons, etc.) and their degradation products. Heterogeneous processes on sulfate aerosols and polar stratospheric clouds (Type 1a, 1b, and 2), and denitrification and dehydration processes are also represented.

[6] The predicted constituents are used in the CAM3 calculations of solar and longwave radiation, and in the nonLTE longwave cooling code above 70 km. Solar heating is calculated using the CAM3 parameterization below 70 km. Over 1 pressure scale height, between 63 and 70 km, the CAM3 shortwave heating is merged with specified (diurnally varying) heating from the Thermosphere Ionosphere Mesosphere Electrodynamics General Circulation Model (TIME/GCM) [*Roble and Ridley*, 1994], as described by *Sassi et al.* [2002]. Therefore, the solar heating is fully interactive with the chemistry below 63 km, but is not interactive above 70 km. The figures below are shown only up to 65 km.

3. Ozone Climatology With Fully Interactive Chemistry

[7] Figure 1 shows the monthly averaged zonal-mean ozone field obtained from the fully interactive chemistry simulation: the field for each month represents a 20-year average. During northern hemisphere winter the combined effects of vortex edge mixing and zonal-mean advection are reflected in mixing ratio isopleths turning upwards around 70N and 25 km, then poleward and downward at about 40 km. During southern winter, the edge of the polar vortex is more marked: at this time the mixing ratio isopleths turn only slightly poleward in the upper stratosphere. In October, significant ozone depletion takes place over Antarctica in the lower stratosphere (15–25 km, poleward of 70S).

0094-8276/05/2004GL022131$05.00

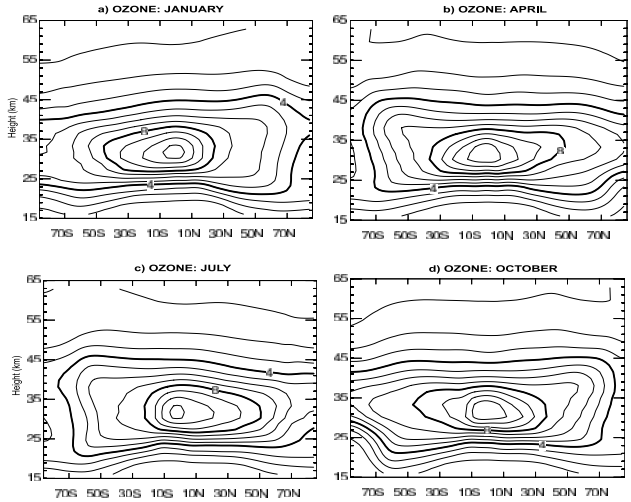

Figure 1. Zonal-mean model climatological ozone obtained from the fully interactive simulation and averaged over 20 years. (a) January. (b) April. (c) July. (d) October. Contour interval is 1 ppmv.

[8] Compared to observations [*Randel et al.*, 1998], the model ozone shows remarkable similarities but also notable differences. Figure 2 shows the ozone difference (model minus observations) calculated for each month shown in Figure 1. The difference plots show that, below about 35 km, the model has a surplus of ozone that is largest in the Tropics ($\sim$1.5 ppmv), but exceeds 0.75 ppmv at all latitudes. This ozone excess is probably due to a deficit of NO_x below 30–35 km (not shown). Large negative differences over the northern hemisphere winter pole throughout the stratosphere – down to 25 km – indicate that the vortex edge is less permeable in the model, and high latitude air is less affected by lateral mixing than in observations. Similarly, negative ozone anomalies around equinox (April and October) result from the late vortex breakup during NH winter, and the early setup of the vortex during fall. Those aspects of model climatology are associated with stronger and more persistent winds in the lower stratosphere that affect the propagation of planetary waves. The differences at high latitudes, however, should be taken with caution because UARS data (particularly observation from HALOE) degrade rapidly toward high latitudes. Finally it should also be noted that WACCM2 has an ozone deficit in the upper stratosphere and lower mesosphere of about -0.75 ppmv ($\sim$15%) compared to observations. The origin of these ozone anomalies is still under investigation.

4. Comparison of the Two Simulations

[9] The ozone climatology presented in Figure 1 is used in the second simulation to compute shortwave heating rates; it is applied as a zonal-mean field with an annual cycle that repeats every model year.

[10] The shortwave heating rate calculated from the fully interactive simulation (not shown) has the largest values in the upper stratosphere of the summer hemisphere. The peak zonal-mean heating rate is about 13 K day^{-1} at solstice. Figure 3a shows the difference (interactive minus non-interactive ozone) in shortwave heating rate between the two simulations. There is a deficit in the interactive simulation of about -2 K day^{-1} in the lower mesosphere, and an excess of about 0.2 K day^{-1} at 45 km. The negative heating rate difference maximizes around 65 km and then decreases upwards (not shown), as we transition to the specified TIME/GCM heating: the occurrence of a maximum at 65 km is almost certainly an artifact generated by the imposition of fixed heating rates from TIME-GCM above 70 km in both simulations. The heating rate difference in the lower mesosphere is a substantial fraction (as much as 50%) of the total shortwave heating.

[11] The heating rate deficit in the lower mesosphere originates from the lack of a diurnal cycle of ozone in the non-interactive simulation. Figure 3b shows the instantaneous (0.0 UT) zonal profiles of ozone at the equator and 60 km from the fully interactive (solid) and the non-interactive ozone simulation (dashed). The fully interactive simulation shows a large diurnal cycle, with larger ozone mixing ratio at nighttime and smaller during the day. On the other hand, the climatological ozone, which was constructed as the zonal mean of the interactive ozone field, is constant regardless of local time. During daytime, when there is heating from the absorption of solar radiation, the mixing ratio of ozone is smaller in the fully interactive simulation, and therefore results in smaller zonal-mean heating rates. Observational climatologies, which are largely based on daytime observations, would not produce this heating anomaly, but would also not represent the increased longwave cooling at night, when ozone is large. The longwave cooling anomaly (not shown) is smaller because longwave cooling is dominated by CO_2 and is primarily a local response [*Dickinson*, 1973].

[12] The heating rate excess around 40 km (Figure 3a) is small but also reflected in the temperature difference (cf. Figure 4). Because of the reduced solar absorption in the lower mesosphere, more shortwave photons reach the upper stratosphere where they are ultimately absorbed, resulting in a positive shortwave heating anomaly.

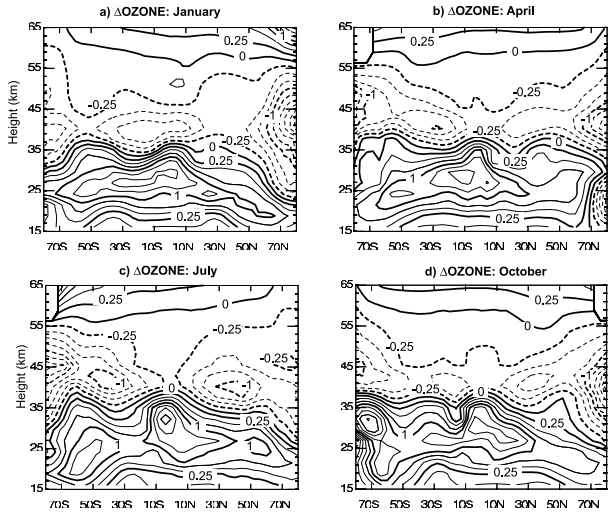

Figure 2. Zonal-mean ozone differences (ppmv) model minus observations (UARS ozone climatology) for (a) January, (b) April, (c) July, (d) October. Contour interval is 0.25 ppmv.

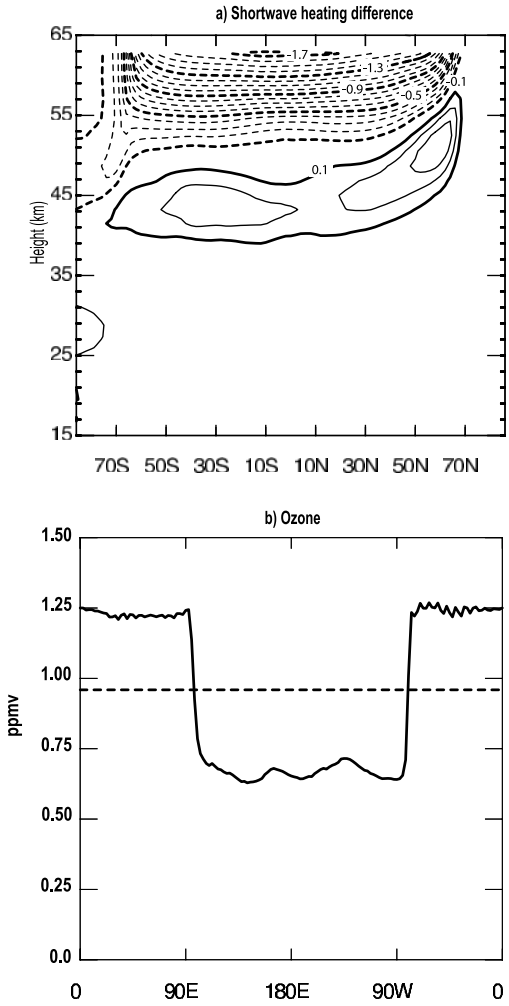

Figure 3. (a) Zonal-mean shortwave heating rate difference (fully interactive minus non-interactive ozone simulations) for January in units of K/day. Contour interval is 0.1 K/day. (b) Instantaneous zonal profile of ozone (ppmv) for a day in January at the equator, 60 km, and at 12 midnight 0E. Solid is ozone from the fully interactive simulation, dash is the zonal-mean climatological ozone in the non-interactive simulation.

[13] We now turn our attention to the climate of the two simulations. The temperature difference is used as an indicator of mean climate difference between the two simulations. The temperature change between the two simulations results in part from the different pattern of absorption of solar radiation. Figure 4 shows the zonal-mean temperature difference calculated from 20-year averages during January, April, July and October. Shadings in Figure 4 indicate those locations where the difference exceeds the 90% significance level based on a t-test with 19 degrees of freedom for each time series.

[14] The negative temperature differences in the lower mesosphere are nearly ubiquitous and reflect the shortwave heating deficit illustrated in Figure 3. These anomalies are broadly statistically significant at all times of the year, except near the winter pole where the variability is large. The positive anomaly in the Tropics of the middle stratosphere is also statistically significant: that pattern is associated with the positive shortwave heating anomaly in Figure 3a at about 45 km.

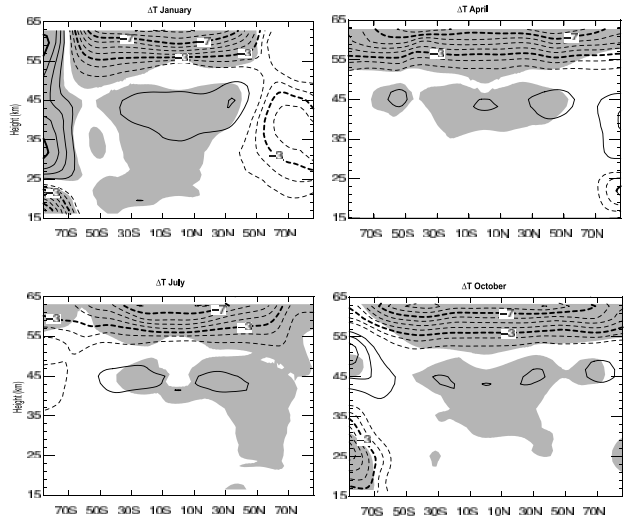

Figure 4. Zonal-mean temperature differences (fully interactive minus non-interactive ozone simulations) for (a) January, (b) April, (c) July, and (d) October. Contour interval is 1 K. Shading indicates locations where the difference is statistically significant at least at 90% level of confidence based on a t-test.

[15] Significant difference patterns are also found near 25 km in the polar stratosphere of the southern hemisphere during October. Warmer temperatures in the non-interactive run result from the way in which the ozone climatology is applied in the non-interactive run. We have specified the ozone distribution in the non-interactive simulation by interpolating linearly between the monthly mean climatological values; although this is a common practice, it has the effect of reducing the amplitude of extrema. Figure 5 shows the composite annual cycle of zonal mean ozone at 88S and 21 km. The daily values (solid curve) show a very rapid decrease of ozone from August throughout October and an equally rapid increase from October to January. The

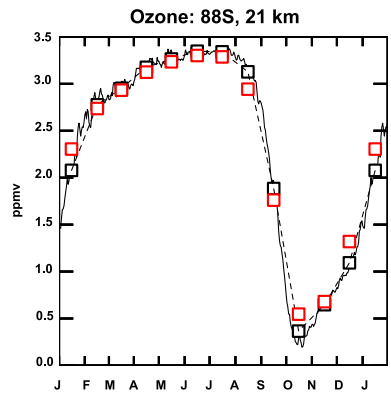

Figure 5. Composite annual cycle of zonal mean ozone (ppmv) at 88S and 21 km: daily values (solid), monthly mean of daily values (black boxes), and monthly mean of the non-interactive model simulation (red boxes). The linearly interpolated values between the monthly mean of the interactive simulation are shown by a dash line.

monthly mean of those daily values (black boxes) misses the minimum values of the ozone hole in October, which lasts only about 2 weeks. This behavior is exacerbated in the non-interactive simulation, where ozone is specified from linear interpolation of the monthly means of the interactive simulation. This is illustrated by the dashed line in Figure 5, which denotes the ozone mixing ratio "seen" by the non-interactive run. It is clear that these ozone values are higher than those in the interactive case, especially in the critical period from late September to mid-November, when the ozone hole is deepest. These high ozone values then give rise to the higher polar temperatures in the non-interactive run. A similar problem occurs when boundary data sets in climate models are interpolated in time [e.g., *Taylor et al.*, 2000], although, to the best of our knowledge, it has never been reported in simulations of the middle atmosphere.

[16] Significant temperature differences at southern latitudes persist throughout southern spring into January. These temperature differences result, via geostrophic balance, in stronger eastward zonal winds in the interactive model, reaching into the lower stratosphere at high southern latitudes in January (not shown). The lower stratospheric temperature anomaly is directly associated with the deeper ozone hole of the interactive simulation (cf. Figure 5), and reinforces eastward winds locally. The presence of stronger eastward winds results in filtering of eastward propagating gravity waves, ultimately causing a westward bias of the momentum deposited by gravity waves and a westward anomaly of zonal mean zonal wind (not shown). This is accompanied, via thermal wind balance, by a warm temperature at high latitudes above 25 km as shown in Figure 4a. It should be noted that this feature could be model dependent, since it arises from a highly parameterized process (gravity wave drag) in the model.

5. Conclusions

[17] We have used a general circulation model (WACCM2) with interactive chemistry to study the effects of ozone chemistry on simulations of the stratosphere. In WACCM2, absorption of solar radiation is fully coupled to the chemistry only up to 63 km; above that altitude, the fully interactive heating is merged with specified heating from the TIME/GCM model until, by 70 km, heating is completely specified from that model. We carried out two simulations: In the first one we used fully interactive chemistry, with ozone calculated and affected by transport and chemistry, and used in turn to calculate heating rates due to absorption of ultraviolet radiation. A climatology of ozone from this simulation is compared to observations. The seasonal cycle is realistic, and a deep ozone hole is produced during southern spring. Some notable differences are an ozone deficit in the model upper stratosphere and an ozone excess in the middle stratosphere. Overall, however, the model climatology is deemed realistic.

[18] We then used the zonal and monthly model climatology from the interactive run as a fixed ozone data set for the second simulation. The model ozone climatology is used only in the radiative heating rate calculations and other radiatively active gases remain interactive. We compare the shortwave heating rates calculated in the two simulations and find a smaller heating rates in the lower mesosphere of the fully interactive simulation. That difference is caused by the zonal-mean ozone field in the second simulation, which is higher during daylight than in the fully interactive simulation, where ozone has a strong diurnal cycle due to photochemistry (with a minimum during the day). Therefore, the use of zonal-mean climatological ozone fields is bound to overestimate the daily mean heating at altitudes where ozone is a prominent shortwave absorber with a large diurnal cycle.

[19] We compared the mean climate of the two simulations using temperature differences as indicators. Accompanying the shortwave deficit in the lower mesosphere, a statistically significant temperature difference is calculated at the same locations, and its overall pattern is essentially independent of latitude.

[20] In the stratosphere, the northern winter meridional gradient of temperature is strengthened in the fully interactive simulation but it is not statistically significant at high latitudes. On the other hand, the pattern at low latitudes is broadly statistically significant and results from an excess of shortwave photons in the interactive simulation that reach the stratosphere due to less mesospheric ozone during daytime.

[21] In the Antarctic lower stratosphere, the interactive simulation produces colder temperature during southern springs that are statistically significant, and continue into southern summer. These differences result from the way the ozone climatology is applied in the non-interactive simulation: by linearly interpolating between monthly means of the climatological data set, the ozone experienced by the non-interactive simulation is larger than in the interactive run between October and January, and leads to warmer temperatures during these months.

[22] The differences between interactive and non-interactive model runs presented in this paper highlight the importance of specifying ozone fields carefully in non-interactive calculations. In particular, the use of monthly and zonally averaged climatologies is inappropriate for ozone, since this species exhibits large diurnal and seasonal changes that are not captured by such averages. Our results show that the common practice [e.g. *Braesicke and Pyle*, 2004] of linear interpolation between monthly means when specifying daily ozone values overestimates ozone in southern spring, when the ozone hole is deepest. This overestimate then produces temperatures in southern spring that are too warm and persist into southern summer.

[23] **Acknowledgments.** The National Center for Atmospheric Research is sponsored by the National Science Foundation. The authors would like to thank the anonymous reviewers for helpful comments.

References

Braesicke, P., and J. A. Pyle (2004), Sensitivity of dynamics and ozone to different representations of SSTs in the Unified Model, *Q. J. R. Meteorol. Soc.*, *130*, 2033–2045.

Dickinson, R. E. (1973), Method of parameterization for infrared cooling between altitudes of 30 and 70 km, *J. Geophys. Res.*, *78*, 4451–4457.

Lin, S.-J. (2005), A vertically Lagrangian finite-volume dynamical core for global models, *Mon. Weather Rev*, in press.

Park, M., W. J. Randel, D. E. Kinnison, R. R. Garcia, and W. Choi (2004), Seasonal variation of methane, water vapor, and nitrogen oxides near the tropopause: Satellite observations and model simulations, *J. Geophys. Res.*, *109*, D03302, doi:10.1029/2003JD003706.

Randel, W. J., F. Wu, J. M. Russell III, A. Roche, and J. Waters (1998), Seasonal cycles and QBO variations in stratospheric CH_4 and H_2O observed in UARS HALOE data, *J. Atmos. Sci.*, *55*, 163–180.

Roble, R. G., and E. C. Ridley (1994), A Thermosphere-Ionosphere-Mesosphere- Electrodynamics General Circulation Model (TIME-GCM): Equinox solar cycle minimum simulations (30–500 km), *Geophys. Res. Lett.*, *21*, 417–420.

Sassi, F., R. R. Garcia, B. A. Boville, and H. Liu (2002), On temperature inversions and the mesospheric surf zone, *J. Geophys. Res.*, *107*(D19), 4380, doi:10.1029/2001JD001525.

Sassi, F., D. Kinnison, B. A. Boville, R. R. Garcia, and R. Roble (2004), Effect of El Nio-Southern Oscillation on the dynamical, thermal, and chemical structure of the middle atmosphere, *J. Geophys. Res.*, *109*, D17108, doi:10.1029/2003JD004434.

Taylor, K. E., D. Williamson, and F. Zwiers (2000), The sea surface temperature and sea-ice concentration boundary conditions for AMIP II simulations, *PCMDI Rep. 60*, 25 pp., Lawrence Livermore Natl. Lab., Livermore, Calif.

World Meteorological Organization (WMO) (2003), Scientific assessment of ozone depletion: 2002, *Global Ozone Res. Monit. Proj. 47*, 498 pp., Geneva.

B. A. Boville, R. R. Garcia, D. Kinnison, and F. Sassi, National Center for Atmospheric Research, P.O. Box 3000, Boulder, CO 80307, USA. (sassi@ncar.ucar.edu)